Monitoring acoustic emission (AE) energy of abrasive particle impacts in a slurry flow loop using a statistical distribution model

Monitoring acoustic emission (AE) energy of abrasive particle impacts in a slurry flow loop using a statistical distribution model

M. G. Droubi[*1], R. L. Reuben[2]

[1] School of Engineering, Robert Gordon University, Aberdeen, AB10 7GJ, UK

[2] School of Engineering and Physical Sciences, Heriot-Watt University, Edinburgh, EH14 4AS, UK

*Corresponding author: Tel: +44 1224 262336, e-mail: m.g.droubi@rgu.ac.uk

Abstract

Slurry erosion has been recognized as a serious problem in many industrial applications. In slurry flows, the estimation of the amount of incident kinetic energy that transmits from particles suspended in the fluid to the containment structures is a key aspect in evaluating its abrasive potential. This work represents a systematic investigation of particle impact energy measurement using acoustic emission (AE), as indicated by a sensor mounted on the outer surface of a sharp bend, in an arrangement that had been pre-calibrated using controlled single and multiple impacts. Particle size, free stream velocity, and nominal particle concentration were varied, and the amount of energy dissipated in the carbon steel bend was assessed using a slurry impingement flow loop test rig. Silica sand particles of mean particle size 225 to 650 μm were used for impingement on the bend with particle nominal concentrations between 1 and 5% while the free stream velocity was changed between 4.2 and 14 ms^{-1}.

The measured AE energy was found, in general, to scale with the incident kinetic energy of the particles, although the high arrival rate involved in the slurry impingement flow loop poses challenges in resolving individual particle impact signatures in the AE record. The results have been reconciled with earlier work by the authors on sparse streams where there are few particle overlaps and good control over particle kinetic energies, by extending their model to account for different particle carrier-fluids and to situations where arrivals cannot necessarily be resolved. The outcome is a traceable methodology whereby a quantitative assessment of particle impingement rate can be made in practical situations.

Keywords: Acoustic emission, particle impact, slurry, abrasive flow.

List of symbols and abbreviations:

AE: acoustic emission

C: solids concentration in flow loop (expressed as weight percentage)

d: Diameter of impacting particle

E_c: AE energy calculated from statistical distribution function model

E_{mean}: Mean of the calibration lognormal pdf of AE energy per particle impact over a fixed time (normally one second) for a specific sensor amplification, $V^2.s$

E_{meas}: Measured AE energy over a fixed time (normally one second) for a specific sensor amplification, $V^2.s$

E'_{meas}: Measured AE energy over one second associated with particle impacts, $V^2.s$

E_w: Measured AE energy over one second associated with particle-free water impingement, $V^2.s$

m: mass of impinging particle

n: curve fit power index, as in $y = Ax^n + B$

n_i: curve fit power index for a particular independent variable (e.g. particle diameter n_d)

$\dot{n}_p$: expected particle arrival rate at target (per second)

r_i: radial position of a particle in a roughly circular impingement area

RMS AE: Root-mean-square of the acoustic emission time series, often used as a time-series itself, of lower effective sampling rate)

t: time (variable)

v: fluid speed in flow loop

v_i: incident velocity of impinging particle

v_p: particle speed in an impinging flow (function of r_i)

$\overline{v_p}$: average particle speed in an impinging flow

$V(t)$: time series amplified AE voltage

wt %: percentage, by weight (for example mass of particles as a percentage of total mass of particles plus carrier fluid)

1 Introduction

Due to the continual need to enhance petroleum production using different reservoir fracturing techniques, loss of pressure in the reservoir and well ageing, there is a consequent increasing likelihood of abrasive particles, such as sand, being present in the hydrocarbon flow at the primary stages of production [1]. This poses serious challenges to the integrity of the production assets, causing thinning of components, surface roughening and degradation, and reduction in functional life, and there is a consequent need to be able to monitor the erosive effect of particle-laden streams on the containment structures (usually pipes). Slurry erosion occurs as a result of interaction between a particle-laden liquid and the containment structure which experiences a material loss due to successive impacts of solid particles travelling at substantial velocities. A number of studies [2-4] have shown a correlation between the rate of dissipated incident kinetic energy due to particle impact and the rate of material removal. Also, amongst researchers in applications of Acoustic Emission (AE) monitoring, there is a general agreement that the AE energy associated with particle impingement is proportional to the incident kinetic energy $\frac{1}{2}mv_i^2$ [1, 5-8], where the relevant mass, m, and velocity, v_i, may be for an individual particle or, more often, an assemblage of particles. Therefore, the measurement of AE energy

associated with particle-laden liquid impingement seems likely to offer a quantitative means of monitoring sand particle impacts and hence slurry erosion.

Studies of the effect of particle impingement parameters on erosion and the effects peculiar to erosion where the carrier fluid is liquid (reviewed in detail elsewhere [7, 9]), have lent impetus to the application of AE as a tool to monitor erosion damage caused by solid particle impacts. Monitoring particle impact using AE is based upon a fraction of the incident kinetic energy of each impacting particle dissipating as elastic waves through the target medium (whose shape and elastic properties affect the propagation characteristics of the signal) before being detected by a suitable AE sensor. Despite the theoretical observation that a relatively low percentage of the incident KE is dissipated in the target as elastic waves (AE), AE has attracted many researchers to examine its potential in monitoring particle impact and slurry erosion. The generated AE signal can be characterised not only on the basis of the particle impact dynamics (which affect the generation of elastic waves in the target medium), but also upon the propagation path of waves through the target and the type and location of the sensors. Therefore, whereas it is a relatively simple matter to establish a correlation between AE and cumulative impact energy in the laboratory, there is a significant calibration problem when it comes to practical application.

One of the seminal studies of hard particle impact on surfaces using acoustic emission was by Buttle and Scruby [10] in which individual glass and bronze particles were dropped freely in a vacuum onto a specimen on whose opposite face an AE sensor was mounted. They concluded that, AE can be used to distinguish particle size provided that the time between individual impacts is at least 1ms. Using a different approach, Boschetto and Quadrini [11] have dropped a predefined weight of powder samples onto a metal plate whilst recording the AE. Different particle materials and size distributions were used, and a normalised number of associated AE counts were measured. Boschetto and Quadrini obtained a simple relationship between AE counts and the mean particle diameter. In an attempt to use AE to estimate the mass flow rates of particles in abrasive jets (controlled to be between 1 and 11 g min^{-1}), Ivantsiv *et al* [12] used glass beads and aluminium oxide powder, in the range of 25-60 μm, and velocities of around 150ms^{-1}, giving particle impacts separated by around 30-100μs. Two approaches were used to estimate the mass flow rate, the first using a dynamic threshold to quantify individual impacts and the second using the power spectral density (PSD) of the AE signal. Also working with high particle arrival rate, but in the quite distinct application of thermal spraying, Faisal *et al* [13] concluded that the measured AE energy can be well correlated with expected kinetic energy.

A few researchers have already assessed AE for its potential for on-line monitoring, carrying out experiments in flow loops and slurry impingement rigs. Duclos *et al* [14] used AE to monitor the impacts of various sizes and concentrations of sand particles borne by water in a flow loop. They observed a general third power correlation between the measured AE energy and the particle diameter, but the energy was lower

than expected for higher particle sizes, which was attributed to particle drop-out according to Stokes' Law. Hou *et al* [15] measured the "acoustic noise" produced by a high concentration slurry of fine silica sand particles (13 μm) flowing in a small diameter flow loop by mounting an AE sensor on the external wall of the pipe. Using both AE signature and stepwise regression analysis, they obtained correlations between the AE and the physical properties of the flow, such as solid concentration, mass flow rate and volume flow rate. ~~Based on the established theory that the main cause of erosion is due to the fraction of impact energy transmitted to the target material, many researchers have attempted to characterize the mechanical damage during the abrasion-corrosion process with the aid of AE measurements and an electrochemical device.~~ Ferrer *et al* [16, 17] have attempted to characterise the mechanical damage due to single and multiple particle impacts by monitoring impingement in a slurry jet rig with an AE sensor coupled onto the back face of a 304L stainless steel target varying the fluid flow rate (1-16 ms^{-1}), particle concentration (1-8 wt%), and angle of impact (30°-90°). They observed a linear correlation between AE energy and particle impact KE, and also showed that the measured cumulative AE energy is proportional to the material weight loss. On this basis, they claimed that acoustic energy may be used to measure a loss of mass due to particle impacts in slurry transport pipelines, although clearly some kind of calibration would be required. Similarly, Oltra *et al* [18] showed that the mechanical wear (measured as a mass loss after the 1 hour erosion test) was proportional to the mean value of RMS AE signal for the duration of the test. Burstein and Sasaki [19], as well as concurring with the observation [18], further indicated that using either the maximum amplitude of individual AE events or the RMS AE value was an acceptable measure of the magnitude of the (wear inducing) impacts in a slurry jet impingement rig.

An essential aspect of AE monitoring is to be able to establish the physical phenomena which generate the AE. In the case of particle-laden flows, the phenomenon of interest is particle impact with the containment walls, although there may well be other sources (such as that caused by turbulent flow) which constitute noise. Ferrer *et al*. [16] demonstrated a relationship between particle launch kinetic energy and AE energy by making measurements on single particle impacts prior to their slurry impingement studies [17], and have published an AE record which purports to show single particle impacts, although it is not clear what impingement conditions were represented. Ukpai *et al*. [20] have also published raw AE records showing what they claim to be single impact events in slurry flows, although they stop short of determining the yield (particle launch rate to impact event rate). Given that both Ukpai *et al*. and Ferrer *et al.* used hit-based AE systems with a threshold, it is possible that many events are lost in the dead time or under the threshold and so calibration would depend somewhat on system settings as well as the many other factors identified above.

The approach in the present work has been to carry out a graded set of experiments where particle impact is initially highly controlled (dropping particles under gravity and with air assist) [7], followed by slurry impingement tests with light and heavy particle loading and various impingement rates [9], to a final series of experiments where the control of particles is limited to controlling the particle density in a flow loop. Throughout these experiments, the same target and sensor arrangement was used so that its propagation properties are built into the calibration of AE energy against impact energy. In addition, full bandwidth raw AE was collected, with all processing being done after acquisition, so that no part of the record is lost. The purpose of this paper is firstly to examine, over a wide range of impact conditions, the relationship between measured AE energy and slurry flow loop parameters, and, secondly, to extend the applicability of the statistical model relating AE energy to particle impact energy described in [21] to relatively uncontrolled impingement experiments where the carrier fluid is a liquid. The ultimate aim is to provide a methodology for quantitative AE monitoring of real process flows.

2 Experimental method

The experimental set-up (**Figure 1**) used an AE system with a carbon steel target assembly identical to those used for earlier tests using an air jet [7] and a slurry impingement jet [9]. The flow loop consisted of a positive displacement pump (model C22BC10RMB, Mono pump driven by a 1.1 kW geared motor to give an output speed of 587 rpm), standard 23 mm PVC piping, a 50 litre conical tank and choke valves. The slurry was first mixed by recirculating it through a by-pass leg for around 20 minutes to ensure that all the solids were suspended in the flow before diverting the flow to the bend.

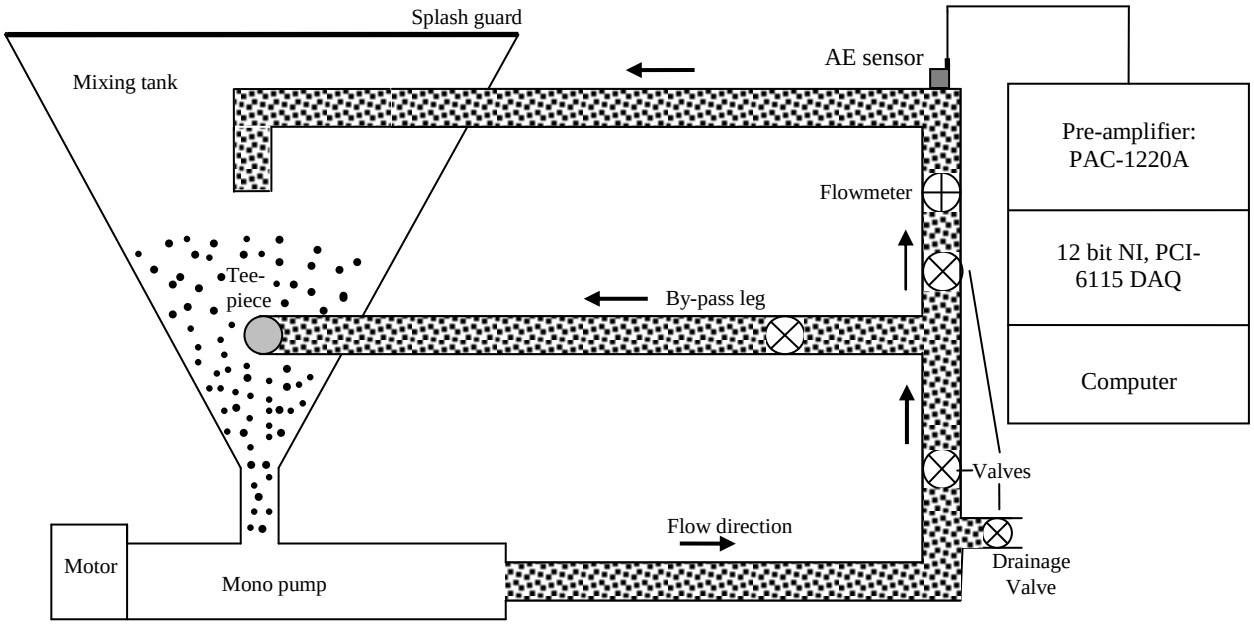

Figure 1: Experimental flow loop and measurement system.

A sharp 90 degree bend made from 5 mm bore carbon steel (**Figure 2**) was inserted into the 23 mm bore PVC pipeline system, a sharp bend having been selected in order to localize the impingement area and minimize the impact angle range. The pipe wall opposite to the stream was milled flat in order to have a plane area to mount the AE sensor and the bend was machined to give an internal bore of 5 mm with a conical transition, giving 7 mm wall thickness at the site where the sensor was mounted. The length of the target section was 75 mm giving an overall impingement area similar to the other studies [7, 9, 21]. A broad band piezoelectric AE sensor (Micro-80D, Physical Acoustics Corp.) was coupled by means of high vacuum grease onto the outside surface of the bend directly above the impingement area then clamped onto the bend using a magnetic clamp. The sensor was 10 mm in diameter and 12 mm in length, and is not truly broadband but produces a relatively flat frequency response across the range (0.1 to 1 MHz) and operates in a temperature range of -65 to 177 ^{o}C. The signal from the AE sensor was pre-amplified (PAC series 1220A with switchable 20/40/60 dB gain and integral band pass filter between 0.1-1 MHz) and AE records were acquired during impingement at a sampling frequency of 2.5 MS/second for a duration of 1 second at full bandwidth. Prior to testing, the sensitivity of the sensor was checked by performing a pencil lead break test [22] at the bend to check the functioning of the AE detection system and to confirm the quality of sensor coupling. The AE energy measured was based on at least ten repeats for each particle size range tested. Following each set of experiments with a given particle loading, the rig was drained and cleaned.

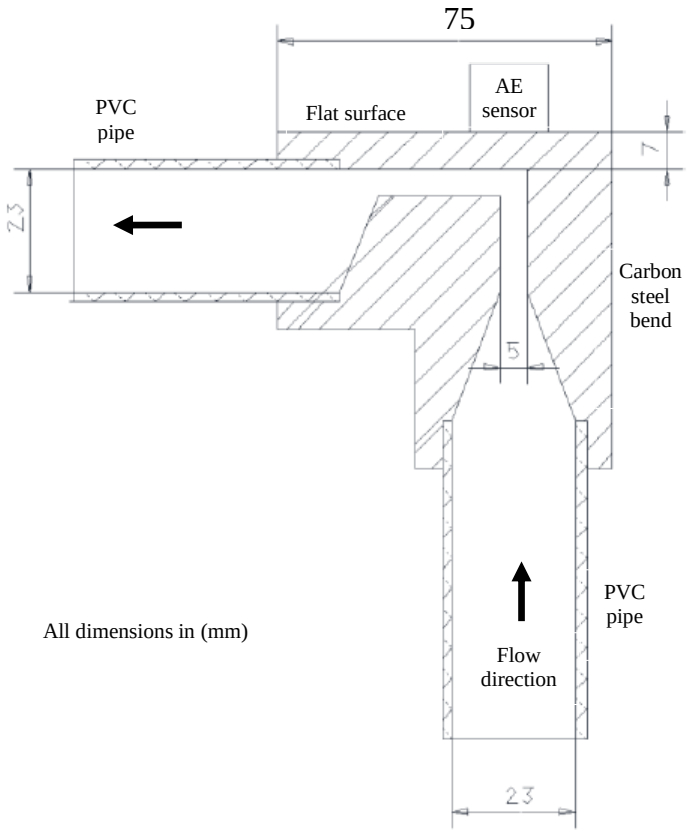

Figure 2: Sectional view of carbon steel bend test section

Silica sand slurry was prepared from 10 litres of clean water and a predetermined mass of different particle size fractions in order to obtain the required concentration. Four different particle size ranges were used and, for each particle size range, an impingement run was carried out with a total of three levels of solid concentration, C, (1, 2.5 and 5 wt%), where wt% is the percentage concentration of solids by weight in the slurry, and four different flow speeds, v, (4.2, 6.8, 10.2, and 12.7 ms^{-1}). The nominal concentration of the particles in the suspension was based on the amount added to the rig, but, for each combination of size fraction, nominal concentration, and flow speed, (**Table 1** shows an example for one size range) the actual sand content of the impinging mixture was measured by sampling the slurry flow at the exit. Ten samples of fixed volume were taken, dried in an electronic oven, and the residual solids weighed, the average of these ten samples being used as the measured concentration. It should be noted here that a significant difference between the nominal and the measured concentration is observed, particularly at lower speed and lower nominal concentration. This might be due to the flow not having sufficient momentum to drag sand as the particle Reynolds number for low speed carrier fluid is low and this will have a proportionately larger effect at low concentrations. The total number of particles per second, $\dot{n}_p$, expected to strike the bend and contribute to AE

energy was determined by multiplying the volumetric flow rate (m^3s^{-1}) by the average measured concentration ($kg.m^{-3}$) and dividing by the average mass of a particle (kg).

Table 1: Summary of derived impingement conditions for flow loop experiments for particles in the size range 300-425µm

Particle size range (µm)	Nominal concentration (kg/m^3)	Flow speed (m/s)	Average measured concentration (kg/m^3)	Average particle impact rate $\dot{n}_p$ (particle/second)×10^3
300-425	10	4.2	1.8 ±1.4	9.2 ±6.99
		6.8	6.2 ±2.1	49 ±16.6
		10.2	6.2 ±2.8	74 ±32.5
		12.7	5.9 ±2.6	88 ±41.3
	25	4.2	10.1 ±2.9	50 ±13.5
		6.8	16.4 ±0.6	130 ±10.9
		10.2	18.4 ±1.9	220 ±24.2
		12.7	14.3 ±5.2	214 ±74.9
	50	4.2	42.7 ±2.3	212 ±21.2
		6.8	51.3 ±2.7	408 ±22
		10.2	52.9 ±6.5	631 ±100.9
		12.7	54.5 ±5.6	812 ±89.3

The background noise AE energy associated with particle-free water impingement and the variability in AE energy associated with sensor removal and replacement between experiments was assessed in three tests between which the sensor was demounted and reinstalled, running clean water at each of the four flow speeds (v). The measured AE energy, E_{meas}, was calculated from the raw time series signal, measured as an amplified voltage, $V(t)$ by integrating over the entire record:

$$E_{meas} = \int_0^t V^2(t)dt \qquad (1)$$

Figure 3 shows the measured AE energy at each of the speeds for each of the three tests where each point represents the average of ten 1-second AE energy values along with its standard deviation. Also, as can be seen, the variation in the energy recorded for each test (the variation of the ten recorded AE energy values at a given speed in a given test) is small, while the variation between tests (the effect of remounting the sensor) is slightly larger. The best power law fit, n, is also shown for each test and, as can be seen, the value is about 2.

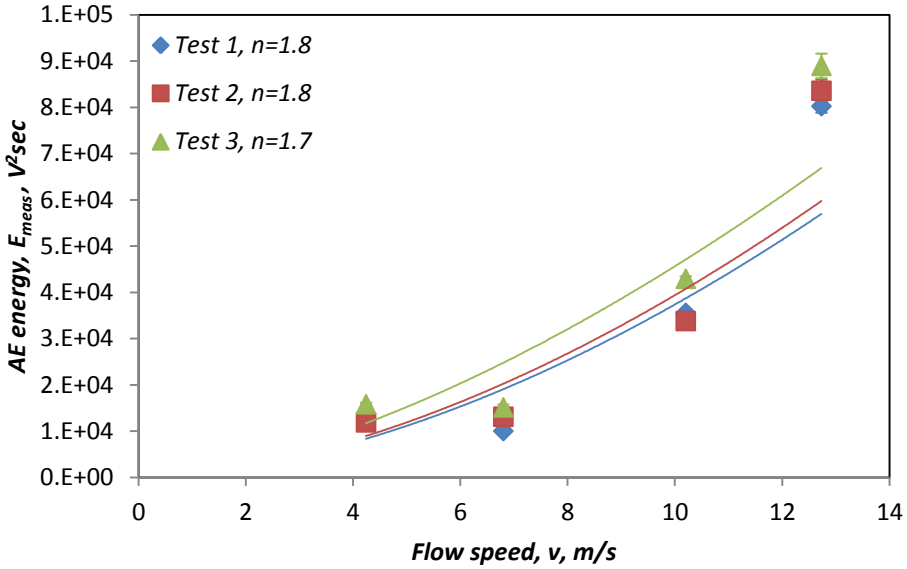

Figure 3: Measured AE energy for particle-free water impingement in flow loop

3 Results

In contrast to earlier work [7, 9], the aim of this set of experiments was to investigate, over a wide range of impact conditions, the dependence of the measured AE energy associated with particle impacts upon the slurry impingement parameters in a way in which it might be deployed in practice.

At least ten repeat 1-second records were analysed for each experimental condition and the average value is used in the following general analysis to establish the effects of flow speed, particle size, and concentration. A few sample plots are also shown to illustrate the general trends in the data and the degree of variation around the average for each point.

The normal expectation would be that energy will depend on the square of the flow (assumed equal to impact) speed, the cube of the particle diameter (i.e. the particle mass) and be linear with concentration, i.e. expected power law indices for impact speed, $n_v = 2$, for particle size, $n_d = 3$ and, for concentration, $n_C = 1$. Accordingly, the variation of the best fit power index for all experiments for each of the variables (n_i) along with their respective correlation coefficients (R_i) were determined by curve-fitting to arrive at the weighted average exponent for each experimental variable, $\bar{n}_i$, calculated from:

$\bar{n}_i = \frac{\sum n_i R_i^2}{\sum R_i^2}$	(2)

Figure 4 shows an example of the effect of the flow speed (v) on the measured AE energy for the maximum particle size range for each of the concentrations (C). Table 2 shows the corresponding best-fit indices, n_v, for this size range (bold type) and the remaining size ranges along with the corresponding R_v^2 values. As can be seen, the flow speed exponent, n_v, is close to the expected value of 2 for all particle size ranges except the lowest size fraction where the signal to noise ratio might be expected to be lowest. The weighted average exponent, $\overline{n_v}$, was calculated from **Equation 2** to be 2.0, which, besides being the expected value, is in reasonable agreement with other studies which report this index to vary in the range of 1.5-3 depending on the slurry properties and mechanical properties of the material under investigation [23].

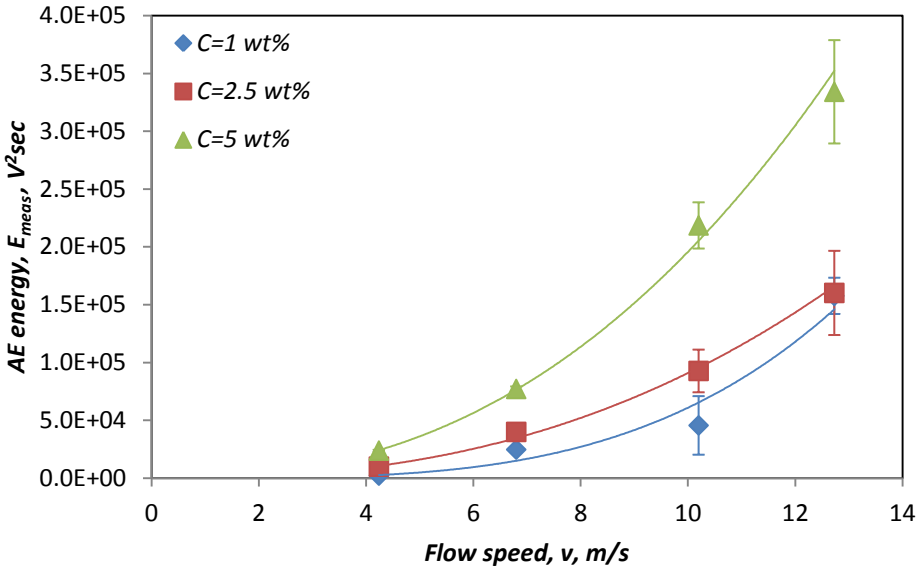

Figure 4: Effect of flow speed, v, on the measured AE energy for the three concentrations, C, for particle size range 600-710 µm

Table 2: Power index of flow speed dependence of measured AE energy and correlation coefficient for all experiments (bold text data are shown in Figure 4)

Particle size range (µm)	Nominal concentration (kg/m^3)	Flow speed power index (n_v)	Curve fitting R_v^2 value (%)
212-250	1	-	-
	2.5	0.45	36
	5	0.63	91
300-425	1	2.5	97
	2.5	1.9	98
	5	2	96
500-600	1	2	88
	2.5	1.8	94

	5	2.2	94
600-710	**1**	**3.6**	**95**
	2.5	**2.5**	**99**
	5	**2.4**	**99**

Figure 5 shows an example of the effect of mean particle diameter on the measured AE energy for each of the flow speeds at the 5 wt% nominal concentration and **Table 3** lists the best fit diameter power index for all measurements, leading to a weighted mean exponent $\overline{n_d}$ of 2.6. As can be seen, generally the energy varies with approximately the third power of the mean particle diameter, except in the case of the lowest speed where there is very little particle signal (above the water "noise") and where changes are difficult to discern at all.

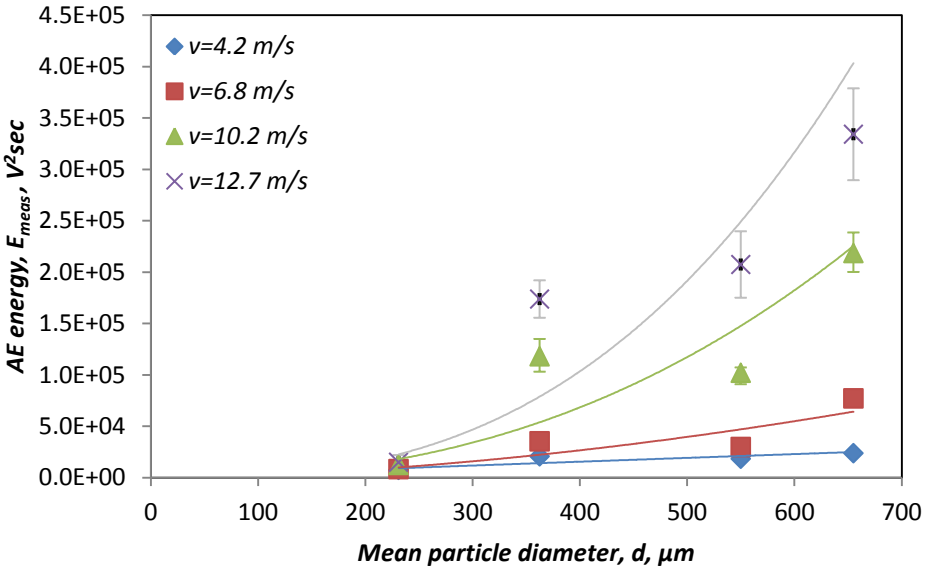

Figure 5: Effect of mean particle diameter, *d*, on the measured AE energy at the four flow speeds, *v*, with a 5 wt% solid concentration

Table 3: Power index of particle size dependence of measured AE energy for all experiments (bold text data are shown in Figure 5)

Nominal concentration (kg/m^3)	Flow speed (m/s)	Particle diameter power index (n_d)	Curve fitting R_d^2 value (%)
1	4.2	0.8	17
	6.8	3.3	97
	10.2	3.8	92
	12.7	4.8	91
2.5	4.2	1.5	79

	6.8	2	97
	10.2	3.2	88
	12.7	3.2	94
5	**4.2**	**0.95**	**74**
	6.8	**1.8**	**81**
	10.2	**2.4**	**80**
	12.7	**2.75**	**85**

Finally, **Figure 6** shows an example of the effect of nominal solids concentration on the measured AE energy for the largest particle size range. Again, **Table 4** summarises the solids concentration power index, n_C, along with curve fitting R^2 values for all the experiments which led to a weighted average, $\overline{n_C}$, of 0.95. Although the weighted average is close to the expected value of unity, Table 3 shows the individual indices to vary in a non-systematic way. Figure 7 shows the average measured solids content for each of the nominal solids contents used in the correlations, including the data for the 300-425µm size range shown in Table 1. Thus, each nominal value has 16 average measured values (4 particle sizes × 4 flow speeds) and each of these values has an experimental error associated with it (see Table 1), the overall average experimental error being about ±20%. In the face of this, the percentage difference between the average of the 16 averages at each of the three solids concentrations is about; a 50% underestimate at 10kgm^{-3}, a 40% underestimate at 25kgm^{-3} and a 0.5% overestimate at 50kgm^{-3}.

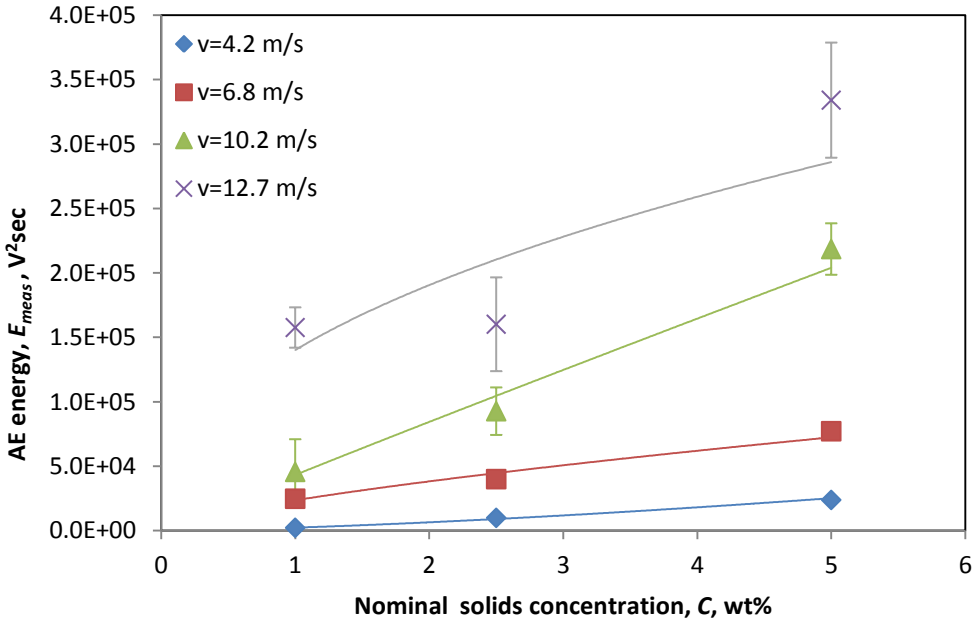

Figure 6: Effect of nominal solids concentration, C, on the measured AE energy for the four flow speeds, v, for particle size range 600-710 µm

Table 4: Power index of solids concentration dependence of measured AE energy for all experiments (bold text data are shown in Figure 6)

Particle size range (µm)	Flow speed (m/s)	Solids concentration power index (n_C)	Curve fitting R_C^2 value (%)
212-250	4.2	0.76	80
	6.8	1.5	95
	10.2	1.6	98
	12.7	1.6	99
300-425	4.2	1.4	99
	6.8	1.1	99
	10.2	1.3	99
	12.7	0.9	82
500-600	4.2	0.25	84
	6.8	0.37	93
	10.2	0.46	99
	12.7	0.3	72
600-710	**4.2**	**1.4**	**99**
	6.8	**0.7**	**97**
	10.2	**1**	**98**
	12.7	**0.45**	**69**

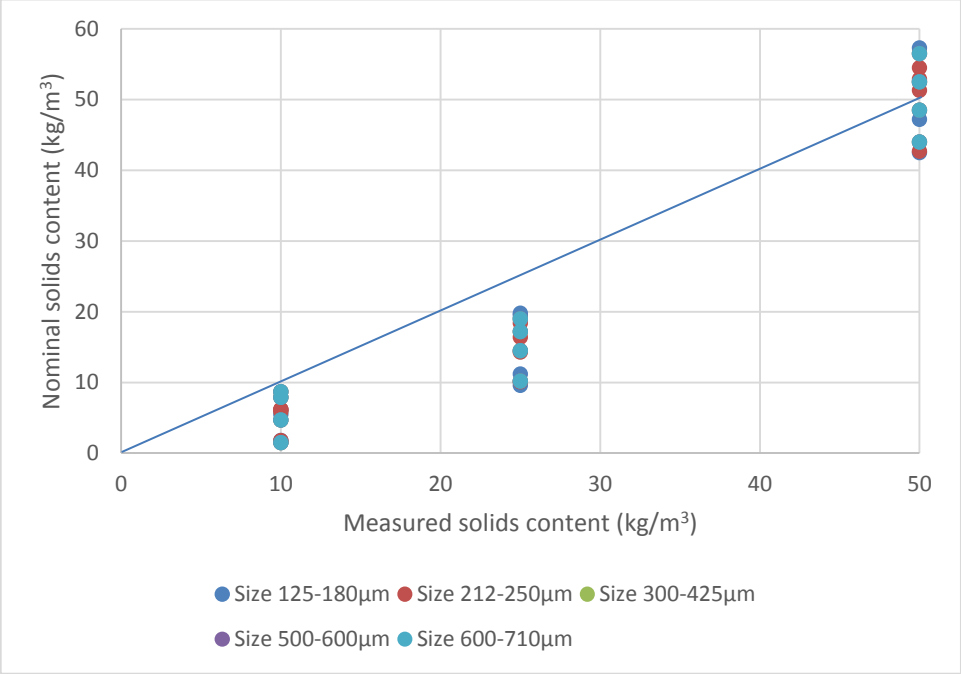

Figure 7: Effect of nominal solids concentration, C, on the measured AE energy for the four flow speeds, v, for particle size range 600-710 µm

4 Discussion

Given that the measured AE energy shows roughly the expected variation with speed, particle density and particle size, it remains to be seen whether the energy measured corresponds to what would be expected from a previously-developed model [21].

The measured AE energy associated with the particles in the fixed record length, E'_{meas}, was estimated by subtracting the background water jet energy E_w from the integral of the signal, Equation (1).

$$E'_{meas} = E - E_w \qquad (3)$$

where E_w was obtained from the average of the correlation functions shown in **Figure 2**.

The lognormal probability distribution of particle impact AE energy for the model was obtained for a range of particle sizes and impact velocities and the model was calibrated against the expected kinetic energy (i.e. nominal mass, m, and nominal speed, v_i, of the impinging particle). The model was then used to describe the probability distribution of particle arrival AE energy for air-propelled particles [7] and slurry impingement [9] using the same target and sensor and the same sensor amplification. The mean of the log-normal probability distribution function of AE energy per particle, E_{mean}, was found to be [21]:

$E_{mean} = 1.7621\, m v_i^2 + 1 \times 10^{-5}$	(4)

As was seen in the authors' previous work [9], there is a discrepancy between flow speed and anticipated particle arrival speed as particles in an impinging jet behave in rather a complex way near the surface. To cope with this, the empirical model, **Equation 4**, of Turenne and Fiset [24] was used to calculate the particle speed, v_p, using the mean particle diameter, d, the flow speed, v. This model is based on actual particle observations in an impinging jet and takes into account the radial position, r_i, of a particle within a circular impingement area. To obtain an average value of the particle speed $\overline{v_p}$, an average value was used for the radial position of a particle (1.25mm).

$v_p = -1.14 + 0.004\, \frac{r_i v^{0.5}}{d^2} + 0.762\, dv$	(5)

Table 5 shows the calculated average arrival speeds $\overline{v_p}$ for all the conditions studied. In some cases of slowly moving particles, the model does not give a positive speed, corresponding to particles that fail to penetrate the squeeze film and so these conditions are omitted from the calibration.

Particle size range (μm)	Flow speed (m/s)	Average calculated speed (m/s)
212-250	4.2	-
	6.8	0.3
	10.2	0.95
	12.7	1.43
300-425	4.2	0.1
	6.8	0.84
	10.2	1.8
	12.7	2.5
500-600	4.2	0.65
	6.8	1.75
	10.2	3.19
	12.7	4.24
600-710	4.2	0.98
	6.8	2.28
	10.2	3.99
	12.7	5.24

Table 5: Calculated particle arrival speed using the model of Turenne and Fiset [24]

The expected AE energy arising from a population of the wet impacts in one second, E_c, can now be obtained by multiplying the average particle arrival rate given in **Table 1** by the mean of the energy distribution function given above, i.e.

$E_c = \dot{n_p} \times 1.7621\, \overline{m v_p}^2 \ + 1 \times 10^{-5}$	(6)

Figure 7 shows the relationship between the calculated AE energy from Equation (6) and the measured AE energy from Equation (3) taking all the data together, i.e. for all particle size ranges, concentrations and flow speeds investigated. This plot shows the extent to which a model developed using only data from particle-controlled experiments can be applied to a case where the particle arrival rate is so high that the individuals cannot be controlled or resolved even with the high temporal resolution offered by full-bandwidth AE monitoring. Given that this plot incorporates all of the experimental error reported in Tables 2-4, the relationship is remarkably consistent (R^2 of around 0.8). The slope is also remarkably close to the ideal value of unity (shown dotted in Figure 7), although there is a systematic tendency for the model to overestimate energy by an average of about 35% (average slope of 1.35). Looking at Equation (6), this could be due to overestimates of the particle arrival rate, the average particle mass or the impact velocity, or all three.

Figure 8 shows the same data as Figure 7, this time segmented between the four particle size ranges and Table 6 summarises the slope and consistency (as R^2) for each of the graphs. Clearly, the consistency is better as the particle size increase, but this is probably due to the smaller particles giving considerably less signal. Perhaps more

importantly, the slope decreases as the particle size range increases. This might partly be explained by particle trajectories around the bend generally having an angle of incidence influenced by the bulk fluid flow (an effect which was absent in the impingement experiments on which the model is based), resulting in a greater proportion of smaller particles having an angle of impact less than 90°, and thus overestimate in the calculated AE energy. Another possible reason might be that the hydraulic differences between the bend and the slurry impingement rig result in a smaller proportion of particles actually striking the target and contributing to AE energy due to a higher degree of particle interaction at or near the surface, resulting in a combination of particle collisions, reduced particle impact velocities and changed impact angles. Also, the effect of the slightly different design of the target at the bend with greater wall exposed area might provide a leakage path for AE energy reducing the amount of measured AE energy. These factors have probably all contributed to the (relatively slight) overestimate in the calculated AE energy and are those which would have to be taken into account in any real application of the technique as they are dependent on the design of the system being monitored.

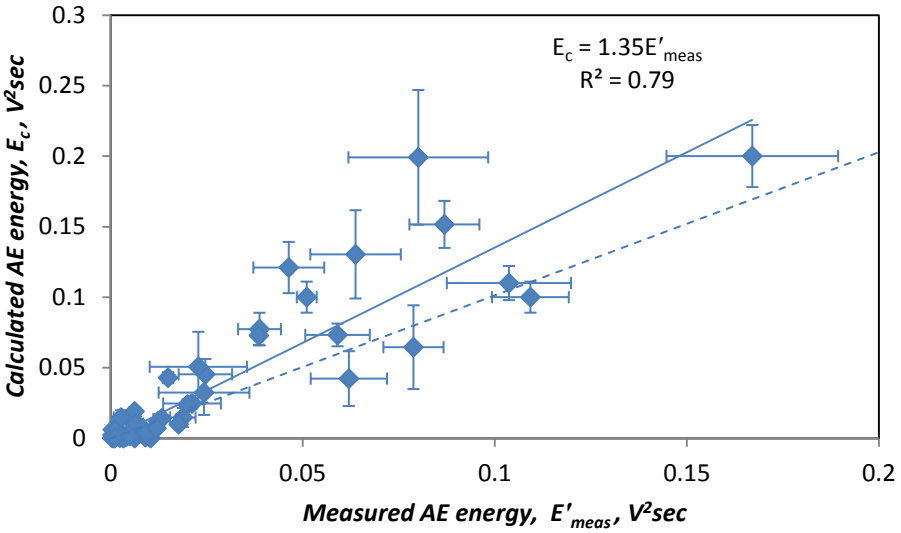

Figure 7: Calculated AE energy, E_c, versus measured AE energy, E'_{meas}, for all particle size ranges investigated. Solid line shows best-fit and dotted line shows ideal where calculated energy equals measured energy.

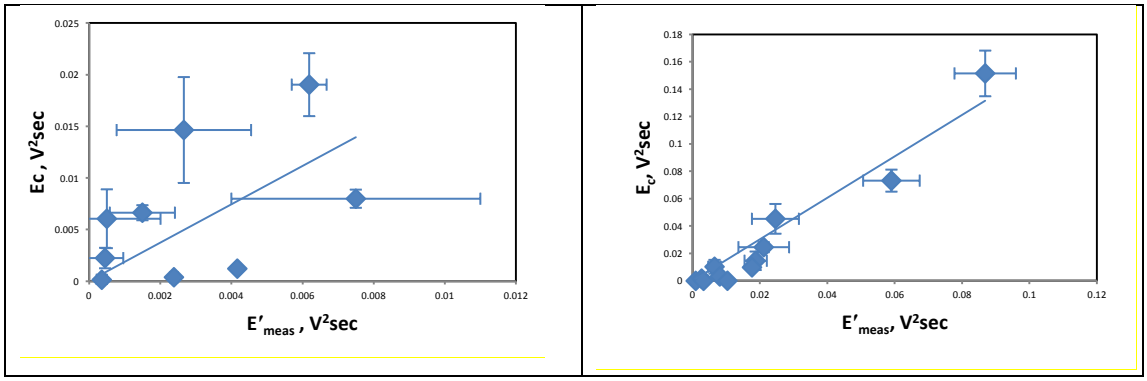

a) Size range 212-250µm	b) Size range 300-425µm
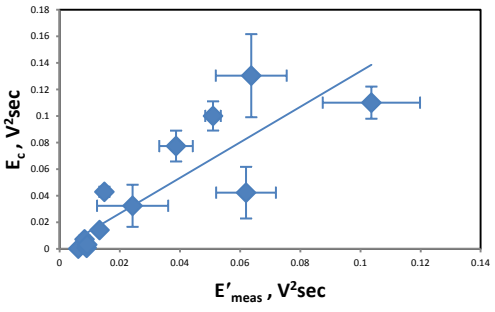	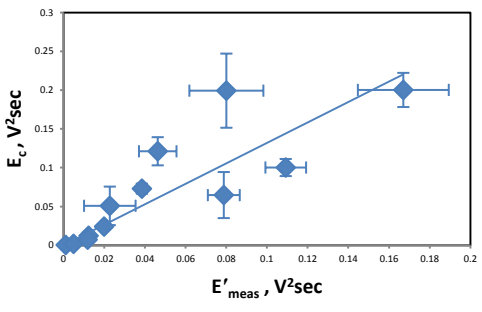
c) Size range 500-600µm	d) Size range 600-710µm

Figure 8: Calculated AE energy, E_c, versus measured AE energy, E'_{meas}, segmented across the four particle size ranges

Particle size range (µm)	Slope	Correlation coefficient (R^2)
212-250	1.8	0.18
300-425	1.5	0.92
500-600	1.33	0.7
600-710	1.3	0.7

Table 6: Summary of fit between calculated AE energy, E_c, Equation (6) and measured AE energy, E'_{meas}, Equation (3).

Thus, a given application on an industrial installation would require the individual monitoring cell(s) to be designed to account for the likely spatial and temporal distribution of sources, as well as options for deployment. Two extreme cases of deployment can be identified, the first where it is feasible to mount an acoustically isolated measurement cell into the pipe wall or where the likely impingement is localised to a predictable area, and the second is where any measurement cell needs to make use of the full pipe wall thickness and the sources may be distributed along and around the pipe for substantial distances. In either case, the principle demonstrated in this work could be used to obtain a quantitative assessment of the impingement rate, expressed as impact energy per unit time. The key to the calibration is to carry out trials with the measurement cell(s) in position where particle impingement is under control and is (preferably) relatively sparse, so that individual impact events can be resolved. In the case of the extended source, the calibration may need to take into account attenuation of impact signals which are more remote from the measurement cell.

5 Conclusions

A series of flow loop tests were carried out with two aims:

- to study the effect of particle size, flow speed, and particle concentration, on the AE energy dissipated in a carbon steel bend, and
- to extend the applicability of a statistical distribution model which allows a direct calculation of particle impact AE energy provided that the target has been calibrated in experiments where the size, arrival rate and impact speed of particles are known as statistical distribution functions.

The following conclusions can be drawn:

1. The measured AE energy was found overall to be proportional to the expected square of velocity, cube of particle size, and linear with concentration of the incident flow over a wide range of particle sizes (125-600 µm), flow speeds (4-12 ms^{-1}), and nominal concentrations (1-5 wt%), but with weaker expression for smaller, slower particles.
2. The calculated AE energy (from the model) showed good agreement with the measured AE energy, but with the model overestimating the energy by about 35% on average, more for smaller particles and less for larger ones. The discrepancies can be attributed to details of the design of the hydraulics and the target, and these are factors which could easily be accounted for in any practical application.
3. The general approach of calibrating a particular target geometry using controlled particle impingement conditions provides a means of quantifying the monitoring of particle-laden streams which goes beyond the simple correlation between process conditions and AE energy, and has distinct industrial as well as research applications.
4. In order to realise a robust measurement in a given installation, it would be necessary to design the measurement cell for the application in question and calibrate this in conditions where the impingement is relatively sparse and also relatively localised so that effects of cell design and through-wall and along-wall attenuation could be taken into account.

References

1. J.W.Martin, BP-Amoco erosional guidelines revision 2.1, 1999
2. Clark H M and Wong K K, *Impact angle, particle energy and mass loss in erosion by dilute slurries.* Wear, 1995, **186-187**(Part 2), pp. 454-464.
3. Tabor D, *The Hardness of Metals*, 1951, Oxford: Oxford University Press.
4. Head W J and Harr M E, *The development of a model to predict the erosion of materials by natural contaminants.* Wear, 1970, **15**(1), pp. 1-46.
5. Burstein G T and Sasaki K, *Effect of impact angle on the slurry erosion-corrosion of 304L stainless steel.* Wear, 2000, **240**(1-2), pp. 80-94.

6. Buttle D J and Scruby C B, *Characterization of particle impact by quantitative acoustic emission.* Wear, 1990, **137**(1), pp. 63-90.
7. Droubi M G, Reuben R L and White G, *Acoustic Emission (AE) monitoring of abrasive particle impacts on carbon steel.* Proceedings IMechE, Part E, Journal of Process Mechanical Engineering, 2012, **226**(3), pp. 187-204.
8. Ferrer F *et al., On the potential of acoustic emission for the characterization and understanding of mechanical damaging during abrasion-corrosion processes.* Wear, 1999, **231**(1), pp. 108-115.
9. Droubi M G, Reuben R L and G. White, *Monitoring acoustic emission (AE) energy in slurry impingement using a new model for particle impact*. Mechanical Systems and Signal Processing, **62-63,** (2015), pp. 415-430.
10. Buttle D J and Scruby C B. *Characterization of particle impact by quantitative acoustic emission.* Wear, 1990. **137**(1): p. 63-90.
11. Boschetto A and Quadrini F. *Powder size measurement by acoustic emission.* Measurement, 2011. **44**(1): p. 290-297.
12. Ivantsiv V, Spelt J K and Papini M. Mass flow rate measurement in abrasive jets using acoustic emission. Measurement Science & Technology, 2009. 20(9) doi:10.1088/0957-0233/20/9/095402
13. Faisal N H A, Reuben R L and Alcock B. *AE monitoring and analysis of HVOF themal spraying process.* Jornal of Thermal Spray Technology, 2011: p. 1-14.
14. Duclos J B, Reuben R L and Steel J A. *A study of particle impacts in fluid flow using acoustic emission*. 2005, Heriot Watt University: Edinburgh.
15. Hou R, Hunt A and Williams R A. *Acoustic monitoring of pipeline flows: particulate slurries.* Powder Technology, 1999. **106**(1-2): p. 30-36.
16. Ferrer F, Idrissi H, Mazille H, Fleischmann P and Labeeuw P. *On the potential of acoustic emission for the characterization and understanding of mechanical damaging during abrasion-corrosion processes.* Wear, 1999. **231**(1): p. 108-115.
17. Ferrer F, Idrissi H, Mazille H, Fleischmann P and Labeeuw P. A *study of abrasion-corrosion of AISI 304L austenitic stainless steel in saline solution using acoustic emission technique.* NDT & E International, 2000. **33**(6): p. 363-371.
18. Oltra R, Chapey B and Renaud L. *Abrasion-corrosion studies of passive stainless steels in acidic media: combination of acoustic emission and electrochemical techniques.* Wear, 1995. **186-187**(2): p. 533-541.
19. Burstein G.T and Sasaki K. *Effect of impact angle on the slurry erosion-corrosion of 304L stainless steel.* Wear, 2000. **240**(1-2): p. 80-94.
20. Ukpai J I, Barker R, Hu X and Neville A, *Determination of particle impacts and impact energy in the erosion of X65 carbon steel using acoustic emission technique*. Tribology International, 2013, **65**, pp. 161-170
21. Droubi M G, Reuben R L and G. White, *Statistical distribution models for monitoring acoustic emission (AE) energy of abrasive particle impacts on*

carbon steel. Mechanical Systems and Signal Processing, 2012, **30**, pp. 356-372.

22. Hsu NN and Breckenbridge FR. Characterisation and Calibration of Acoustic Emission Sensors. Materials Evaluation. 1981; 39: 60 - 8.
23. Laitone J A, *Aerodynamic effects in the erosion process.* Wear, 1979, **56**(1), pp. 239-246.
24. Turenne S, Fiset M and Masounave J, *Effect of sand concentration on the erosion of materials by a slurry jet*. in *Proceedings Wear of Materials - 1989*, Denver, Co., USA.